Predicting Radical−Molecule Barrier Heights: The Role of the Ionic Surface

Neil M. Donahue,* James S. Clarke, and James G. Anderson

Department of Chemistry and Chemical Biology, Harvard University, Cambridge, Massachusetts 02138

Received: December 2, 1997; In Final Form: March 19, 1998

We present a theory of radical−molecule abstraction reactions based on the crossing of reactant ground and ionic states at the transition state. By calculating the evolution of ground- and ionic-state energies as the reactants approach each other, we are able to specify the boundary conditions for an avoided curve crossing problem as the atom is transfered. The lower the ionic-state energy, the lower in energy the transition state will be. This drives strong correlations between barrier heights and the difference of ionic- and ground-state energies. This theory successfully explains the evolution of barrier heights in a series of reactions involving alkanes and several radicals (OH, O, H, F, Cl, Br), in which barriers range from 0 to 10 kcal/mol. A perturbation treatment of the ionic- and ground-state energies improves the performance of the theory. We compare predicted curve-crossing heights with observed barriers for both our theory and for the covalent (singlet−triplet) curve-crossing theory. We also compare observed barriers with reaction enthalpy. Only the ionic curve-crossing theory can simultaneously explain both radical and molecule reactivity.

Introduction

Chemical reactivity, the role of fundamental mechanisms that dictate the kinetics of chemical transformations, is central to developments in modern chemistry across a range of emerging disciplines. A particularly important class of these reactions involves radical−molecule pairs. These reactions draw attention both because of their involvement in the rate-limiting steps of mechanisms controlling DNA repair, aging processes in organisms, catalytic destruction of ozone, etching of microcircuits, photochemical oxidant formation, combustion, etc., and because they span many orders of magnitude in reaction probability per collision. Thus they are of considerable practical and theoretical interest.

An understanding of radical−molecule reactivity currently emerges from three distinguishable perspectives. The first is through direct observation. Notable examples for radicals include flash photolysis,[1−3] crossed molecular beams,[4−6] and discharge flow.[7−12] The second is through electronic structure calculations that are used to calculate reaction potential energy surfaces, including barrier heights, using increasingly appropriate Hamiltonians and very large basis sets.[13−15] The third is through the use of molecular orbital analysis, a pursuit that involves frontier orbitals, avoided curve crossings, delocalization, electron promotion, selected electronic structure calculations, etc., with an eye on understanding specific mechanisms that dictate barrier heights, entropic constraints, etc.[16−20]

Our objectives in this paper are born of a need to develop a context within which we can both understand and predict the reactivity of radical−molecule combinations involving electronically complex systems containing, for example, sulfur, chlorine, bromine, iodine, oxygen, carbon, and nitrogen. We seek connections between the structure of reactants (including symmetry, virtual states, available orbitals, polarizability, electron affinity, etc.) and the enthalpic and entropic barriers to reaction. Connections between reactant wave functions, product wave functions, and wave functions describing the transition state are sought such that each may be understood in its own right and that their relationship can be used to pose boundary value problems that test which surface or surfaces control the reaction probability. A framework for understanding this important class of reactions—a framework for testing hypothesis against observations—must satisfy the following criteria: (a) it must provide a link between the structure of reactants, the structure of products, and a prediction of barrier heights for radical−molecule combinations involving complex substituents, (b) it must diagnose reactivity trends within a homologous series, a series of a single molecule reacting with a manifold of radicals as well as a single radical reacting with a manifold of molecules, (c) it must differentiate between direct and indirect reactions, capturing the propensity of radical−molecule reactions to exhibit multiple transition states, (d) it must be reversible; the reverse reaction shares a common transition state (or series of transition states) with a barrier (or barriers) higher or lower by the reaction enthalpy, and (e) it must facilitate the use of electronic structure calculations of tractable scope by establishing a coordinate system that isolates the mechanisms fundamental to barrier height control.

In this paper we present a theory of radical−molecule reactivity drawn from two of the three perspectives noted above: the use of direct observations and the use of molecular orbital analysis. We present a context defining barrier height control based on the proposition that the total wave function at the transition state, constrained by the Pauli exclusion principle, demands involvement of an excited state,[16,19] into which an electron must be promoted to enable a reaction. We argue that for a large set of gas-phase radical−molecule reactions, the state into which the electron is promoted is an ionic state. Thus, radical−molecule barrier heights are controlled by the interaction of the ground state and an ionic state of the reactants. For atom-transfer reactions the abstraction barrier is an avoided curve crossing of these two configurations as the atom is passed from one radical to the other. The height of the curve crossing is directly and easily related to the ionic energy of the separated reactants (IP−EA of the molecule and radical).

* Corresponding author.

S1089-5639(98)00372-7 CCC: $15.00 © 1998 American Chemical Society
Published on Web 05/14/1998

Our conviction that the ionic surface plays a controlling role in most radical−molecule reactions is based on experimental evidence and in particular on the failure of reaction enthalpy correlations to provide empirical insight into reactivity. Many systems show the influence of the ionic-state energy on the reaction coordinate. Correlations of reactivity with molecular ionization potential are well established,[10,21] while over the years work from this lab has demonstrated the role of radical electron affinity and the wide applicability of an empirical IP−EA reactivity trend with systems including radical reactions with halogen molecules[22] and Cl atom transfer from ClNO.[23]

Theoretical treatments of radical−molecule reactivity emphasize the role of covalent interactions in covalent reactions and almost universally begin the problem by considering the energetics associated with breaking and forming bonds. It has been clear since the work of London[24] that avoided curve crossings control atom-transfer barriers. Subsequent treatments,[20,25−29] for the most part have been based on a valence-bond model of the breaking and forming bonds. Earlier work focused on the role of reaction enthalpy as a governor of barrier heights, while more recent treatments are based on the energetic splitting between bonding and antibonding states in breaking and forming bonds. The valence-bond models[20] do recognize a role for ionic states in the configuration mixing (the avoided crossing) stabilizing the barrier, but the ionic contribution is treated as a perturbation. We contend that the data, however, indicate that the ionic interaction is first-order, with other factors (reaction enthalpy, etc.) acting as perturbations.

This is more than an academic issue. It affects how one thinks about chemical reactivity and affects the order in which one confronts possibly important reactions in complicated chemical systems, such as those mentioned in the opening paragraph. If one considers reaction enthalpy to be the driving force of barrier control, one rapidly makes serious errors in estimating radical reactivity; for example, N atoms should be a major sink for atmospheric ozone. Changing one's perspective to the singlet−triplet splittings in these systems does little to solve the problem, while focusing on the ionic properties of the radicals and molecules provides the correct insight.

Theories of Barrier Height Control

We shall examine three theories of radical−molecule reactivity, focusing in particular on how reaction barrier heights vary from reaction to reaction. Our goal is to identify a critical intersection between these theories and experimental observations in order to test their predictive power. Each theory seeks to relate properties of the separated reactants to the barrier height, and they are differentiated by what is considered the most important controlling property (reaction enthalpy, the splitting between bonding and antibonding states, and the splitting between neutral and ionic states). We shall focus on direct atom-transfer reactions of the basic form

$$\mathrm{AH} + \mathrm{B} \rightarrow \mathrm{A} + \mathrm{BH} \tag{1}$$

where the breaking and forming bonds are essentially two-electron covalent bonds. These reactions reduce to a three-electron problem and constitute the simplest form of radical−molecule reactions. Our figure of merit will be the ability to predict variations in reactivity at the lowest level of perturbation. We stress, however, that our approach is appplicable to a far broader domain than H atom abstraction.

Avoided Curve Crossings. Without question, potential barriers along an atom-transfer reaction coordinate correspond to curve crossings.[30,31] Before treating the specifics of the theories, we shall present the simple geometric result for the curve-crossing height and resonance energy.[20] We assume that the diabatic-state energies evolve linearly over an extended distance in order to simplify the problem. Though such a drastic assumption clearly affects the absolute crossing energies, it will not significantly influence the trends in those energies, except for a multiplicative constant. The crucial concept is to relate properties of the separated reactants and products to boundary conditions of the curve-crossing problem. The critical parameters are the energy gaps for the reactants and products (ΔE_R and ΔE_P) and the enthalpy of the reaction, ΔH. As shown in Figure 1, the curve-crossing energy will be

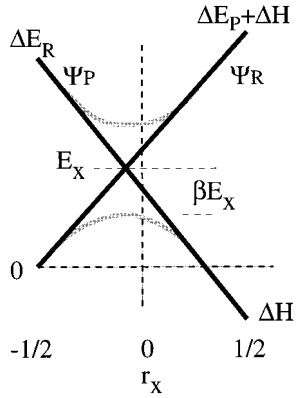

Figure 1. Geometry of curve-crossing problem. ΔE_R is the reactant energy gap, ΔE_P is the product energy gap, and ΔH is the reaction enthalpy. The reaction coordinate r_X is 0 at the midpoint of a symmetric reaction. The interaction of the two diabatic wave functions ψ_R and ψ_P produces a splitting, $B = \beta E_X$, which stabilizes the transition state.

$$E_X = \frac{\Delta E_R(\Delta E_P + \Delta H)}{\Delta E_R + \Delta E_P} \tag{2}$$

For systems with similar wave functions but different energy gaps, the resonance energy splitting the two adiabatic curves ($B = \langle \Psi_P | \hat{H} | \Psi_R \rangle$) at the crossing point will be roughly proportional to the crossing height ($B = \beta E_X \propto E_x \langle \Psi_P | \Psi_R \rangle$). Therefore, we expect the adiabatic reaction barrier to be proportional to the crossing height.

$$E_b = (1 - \beta) E_X \tag{3}$$

In this paper we shall compare predicted curve crossing heights to measured activation energies; the resulting slope will be a measure of the coupling strength, β.

$$\partial \mathrm{E_b} / \partial E_X = (1 - \beta) \tag{4}$$

For most systems, the energy gaps are much larger than the reaction enthalpy. They also tend to vary more from system to system. Therefore, the excited-state energies and not the reaction enthalpy should be the more important controlling factors. Furthermore, the crossing height is essentially the geometric mean of the gaps, so the lower energy gap dominates the crossing energy.

Marcus Theory. By far the most familiar theory of barrier-height control originated with Evans and Polanyi;[25] the essential picture is that an atom-transfer barrier is found at the intersection of two potential curves corresponding to a breaking and a forming bond. Barrier heights vary proportionally with the reaction enthalpy. The most widely used form of this theory was developed by Marcus, first for electron-transfer reactions in weakly coupled systems,[27] but later for strongly coupled

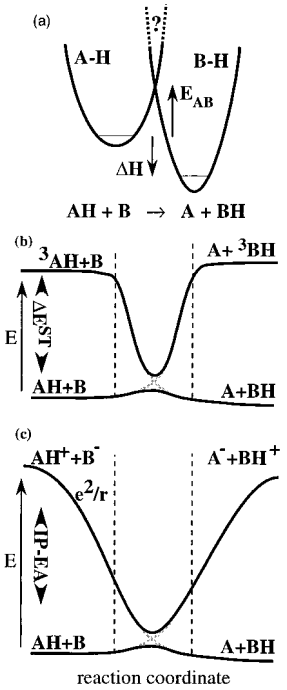

Figure 2. Contrasting pictures of atom-transfer barriers. (a) Marcus theory. The reaction coordinate is modeled as two intersecting parabolic surfaces, with the barrier depending on the enthalpy of reaction and an intrinsic barrier defined by corresponding (thermoneutral) identity reactions. (b) Covalent (Heitler−London) avoided curve crossing. The barrier depends on the singlet−triplet gaps of the breaking and forming covalent bonds. Rapid evolution of the energies begins when orbital overlaps become significant. (c) Ionic avoided curve crossing. The barrier depends on the ionic (electron-transfer) energy of the reactants and products. The ionic energies evolve as e^2/r in the far field.

systems, including atom-transfer reactions.[28] The model, depicted in Figure 2a, is clear: reactants and products are modeled with harmonic potentials, and the reaction barrier corresponds to the crossing of two parabolic surfaces, one for the reactants and one for the products, along a generalized reaction coordinate. When the systems are weakly coupled, the barrier is the curve-crossing energy itself, while, when the systems are strongly coupled, as with radical−molecule reactions, the barrier is lowered by the coupling energy.

The essential characteristic of Marcus theory is that the barrier is assumed to depend on a single extrinsic parameter: the free energy release, which is the "motive force" of the reaction.

$$E_{AB} = E(1 + \Delta E^0/E)^2/4 \tag{5}$$

where E_{AB} is the barrier for the reaction in eq 1, ΔE^0 is the free energy release, and E is the average of the (intrinsic) barriers for the two corresponding identity reactions:

$$E = (E_{AA} + E_{BB})/2 \tag{6}$$

The presence of the intrinsic barrier makes Marcus theory relatively difficult to test. However, the general principle stated by Evans and Polyani[25] is easy to test; changes in barrier heights should be proportional to changes in reaction enthalpy as long as the central atom remains the same.

Covalent Curve Crossings. The second theory originates in the valence-bond formalism presented by London, which has been extended to describe a wide range of chemical systems,[13,20,29,32] including hydrogen atom transfers. This theory recognizes the critical role of excited electronic states in forming the reaction barrier and treats their evolution along the reaction coordinate. For neutral atom-transfer reactions like eq 1, the problem reduces conceptually to a three-electron problem involving doublet surfaces (one unpaired electron). However, the states participating in the avoided curve crossing correspond to the molecular singlet and triplet states when the radical species are far from the molecule. The antibonding triplet state of the reactant molecule correlates with the radical doublet to form a bonding singlet state in the product molecule, and vice versa (^{1}AH → ^{3}BH, ^{3}AH → ^{1}BH). The ionic, or transferred, electronic states are treated as perturbations to the fundamental interaction. The formalism itself is complete and general and, as such, will describe all chemical systems. We shall focus here on the specific simplification that the singlet−triplet curve crossing describes the zero-order behavior of neutral reactions, also called spin-transfer reactions.[20,32]

Because both fundamental states are neutral, their energies remain essentially unchanged as the reactants approach until significant overlap develops between the orbitals of the two reactants. After this, the energies evolve rapidly. Several useful approximate treatments allow us to write a zero-order expression for the curve-crossing height. The functional form first presented by Sato[26] for H_2 was extended by Garrett and Truhlar[33] to a series of H atom transfer reactions. In this form, the singlet−triplet energy gap is

$$E^{ST} = \frac{5 - \Delta}{2(1 + \Delta)} D_0 \tag{7}$$

where Δ is an overlap term generally slightly less than 0.2. For $\Delta \simeq 0.2$, the gap is approximately $E^{ST} \simeq 2D_0$. However, the appropriate energy gap for the curve-crossing problem is[34]

$$\Delta E = 0.75E^{ST} \simeq 1.5D_0 \tag{8}$$

From this we can easily obtain from eq 2

$$E_X = \frac{1.5D_{0R}(0.5D_{0P} + D_{0R})}{1.5D_{0R} + 1.5D_{0P}}$$

$$= \frac{(D_{0R} + 0.5D_{0P})}{1 + D_{0P}/D_{0R}} \tag{9}$$

The theory thus predicts a strong dependence of barriers on the reactant molecule bond strength, with a secondary dependence on the product molecule bond strength. The dependence on the product bond strength is somewhat damped because the product energy gap partially compensates for changes in product bond strength; stronger bonds also have larger singlet−triplet splittings, so the product boundary conditions are anticorrelated. Variations in the singlet−triplet splitting from the simple form in eq 8 constitute a perturbation to the zero-order behavior described here.

Ionic Curve Crossings. Here we present a theory in which an ionic surface interacts with the neutral ground state surface for both reactants and products, corresponding to Figure 2c. This theory has its origins in the harpoon mechanism,[4] which describes reactions where the ionic surface crosses the ground state at an extended impact parameter ($r \sim 7$ Å), leading to the formation of an ionic collision complex and a very large collisional cross section. While the role of the ionic surface in harpoon reactions is well established, the ionic configuration enters into the covalent model presented above only as a perturbation. We hold the opposite view; in many cases the ionic surface couples most strongly with the ground-state surface of the reactants (and products), and the molecular triplet

configuration appears as a perturbation. We shall show that this leads to a profoundly different way of thinking about radical molecule reactivity than the paradigms based on either reaction enthalpy or singlet−triplet splitting.

The zero-order ionic curve-crossing model is easily described. The initial ionic-state energy is roughly equal to the (smaller) difference in ionization potential and electron affinity of the two reactants. As the reactants approach, the ionic surface drops in energy according to a simple Coulombic potential, i.e. $E^I \simeq \mathrm{IP} - \mathrm{EA} - e^2/r$. After significant overlap develops between the reactant wave functions, the simple asymptotic behavior of the energies breaks down and the reaction complex becomes a single species characterized by a molecular wave function. Here we assume that the two lowest energy doublets associated with this complex establish the boundary conditions for a curve crossing such as the one shown in Figure 1 ($AH + B \rightarrow BH^+ + A^-$, $AH^+ + B^- \rightarrow BH + A$). The linear curve-crossing problem (eq 2) is thus

$$E_X = \frac{(\mathrm{IE_R} - E_R^i)(\mathrm{IE_P} - E_P^i + \Delta H)}{((\mathrm{IE_R} - E_R^i) + (\mathrm{IE_P} - E_P^i))} \qquad (10)$$

where the ionization energy IE = IP − EA, and the Coulombic term (to zero order) $E^i = e^2/r$. At this order, we must choose a typical interaction distance for the boundary condition. The zero-order interaction distance is the separation between the heavy centers (R and X) at the transition state. It is typically constant for a given radical but varies slightly from radical to radical depending on the size of the frontier orbital (SOMO) of the radical.

Testing the Theories

The three theories under consideration all represent zero-order conceptual pictures of chemical reactivity. Each is an approximation to the true behavior, and all will converge at higher order. For instance, Marcus theory and the valence-bond picture are closely related, and the singlet−triplet and ionic curve-crossing theories represent different choices about what to regard as a zero-order interaction and what to regard as a perturbation. However, they lead to very different perceptions of reactivity and barrier-height control. We must choose both a method of comparison and a set of reactions to use as a test case.

Choosing a System. We shall compare the theories for an important set of reactions: hydrogen atom transfers from an alkane to an attacking radical. We choose this set because these reactions play a critical role in organic chemistry, combustion, and atmospheric chemistry and because this system has been treated in the context of the first two theories, by Marcus[28] for Marcus theory and by Pross[35] for the valence-bond curve-crossing theory. Also, the experimental data set is large. Our analysis of the available data is presented in the Appendix.

It is critically important to treat reactions involving both a series of alkanes and a series of radicals, as the three controlling properties under consideration (reaction enthalpy, singlet−triplet splitting, and ionic-state energy) are strongly correlated for the alkanes. This is illustrated in Figure 3, which compares the ionization potential and bond strength of a series of alkanes. Any simple correlation treatment of reactivity exploring only a series of alkanes will therefore perform equally well for any of the three theories. The situation is far different, however, when one compares radical electron affinities with radical−hydride bond dissociation enthalpy (Figure 3b). Here the correlation breaks down entirely; for one sequence, the halogens, the electron affinity remains constant while the bond strength varies

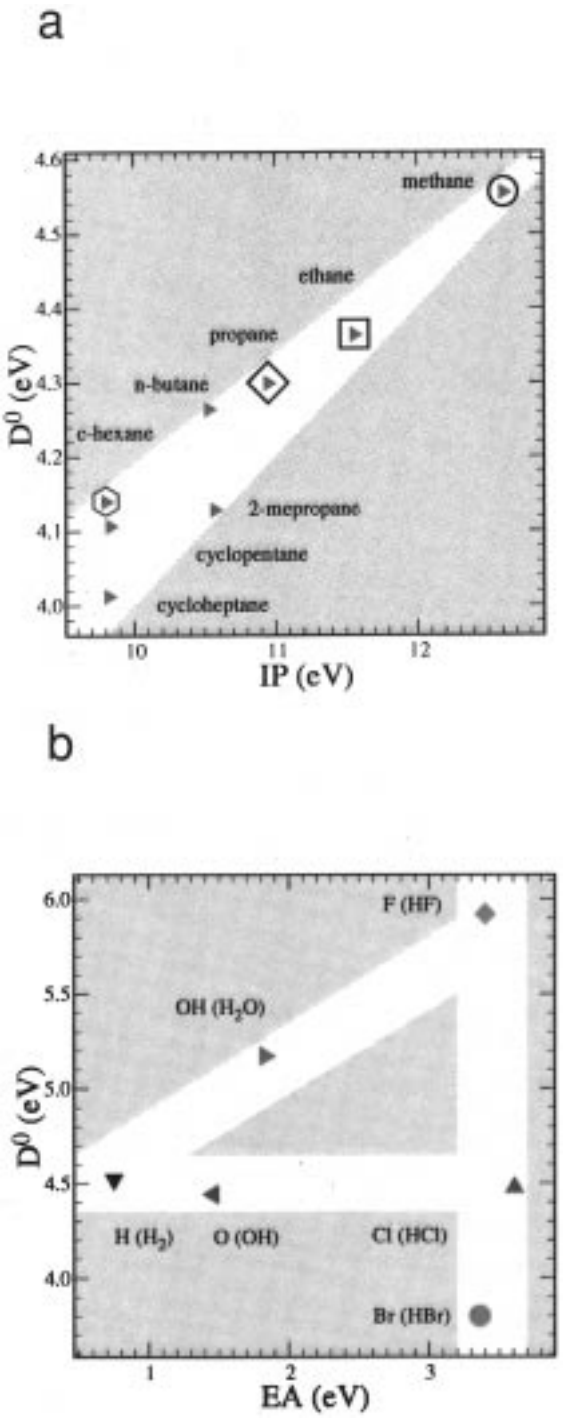

Figure 3. (a) Correlation between ionization potentials and bond dissociation enthalpies for a series of alkanes. The range in ionization potentials is ∼3 eV, while the range in bond strengths is ∼0.6 eV. The open symbols surrounding methane (circle), ethane (square), propane (diamond), and cyclohexane (hexagon) will be used throughout the paper to identify these species. (b) Relationship between electron affinities of radicals and the bond dissociation energies of the associated hydrides. Note in particular that EA for the halogens remains essentially constant as the hydride D_0 changes by 2 eV, while the EA for the series (H, O, and Cl) varies by 2 eV as the associated D_0 stays constant. The color and symbol shape identifying each radical will be used throughout the paper.

by 2 eV, whereas for another (H, O, Cl), the bond strength remains constant while the electron affinity varies by 2 eV.

There is, however, one significant difference between the ionization potential and the bond strengths; the absolute variation in ionization potential is more than a factor of 5 greater than

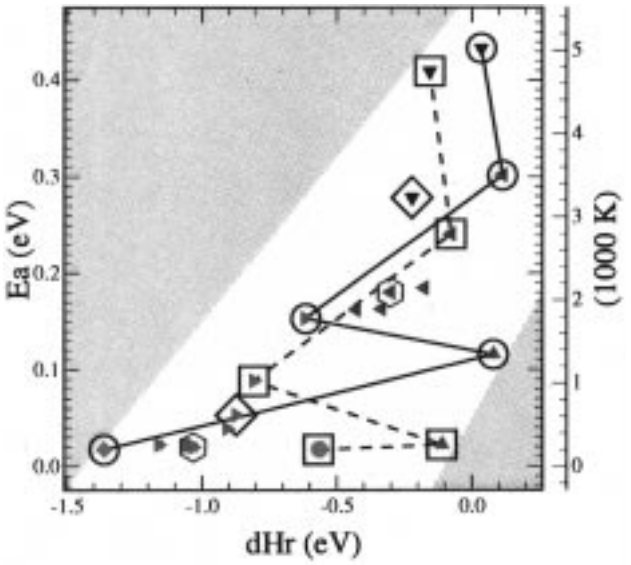

Figure 4. Observed barrier heights vs reaction enthalpy. Symbols identify reactions as in Figure 3. Barriers for a series of alkanes reacting with one radical form a trend, but there is no correlation between reaction enthalpy and radical reactivity, for instance for radicals reacting with methane (open circle, solid line) and ethane (open square, dashed line).

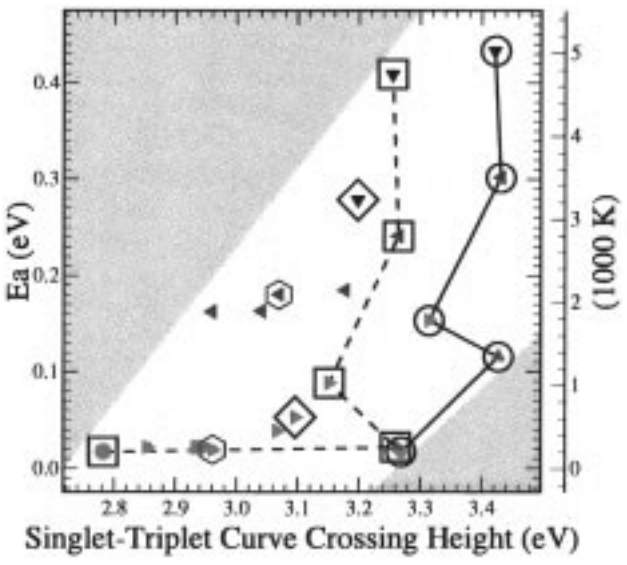

Figure 5. Observed barrier heights vs calculated singlet−triplet curve-crossing energies. Symbols identify reactions as in Figure 3. The experimental barrier heights correlate with the singlet−triplet gap for a series of alkanes reacting with one radical, but not at all for a series of radicals reacting with a single alkane.

that in bond strength, and even the fractional variation is more than a factor of 2 greater. The reason is that the ionization potential is a molecular property, so it is possible to ionize larger alkanes by removing an electron from the highest occupied molecular orbital (HOMO) while leaving the much more tightly bonding electron density of the lower lying orbitals essentially intact. This represents an essential and testable difference between a molecular-orbital construction of the reactants and a valence-bond construction. Therefore, we shall also be able to compare the fractional change in predicted crossing heights with the fractional change in observed barriers as a secondary figure of merit as we test these theories.

Marcus Theory. In the paper extending Marcus theory to tightly coupled systems,[28] Marcus uses hydrogen atom transfers to test the theory. The test is, however, a comparison of BEBO calculations with eq 5. Predictions of both theoretical treatments agree modestly well with one another but fail to reproduce observed trends. Explicit testing of Marcus theory is challenging because it requires measurements of symmetric cross reactions; however, it has been done. Kreevoy and Truhlar[36] showed that the observed rate of the OH + HCl reaction is inconsistent with constraints provided by the cross reaction H + H_2 and Cl + HCl, while Dubey et al.[37] recently measured the symmetric reaction OH + H_2 O → H_2O + OH and found that eq 5 was unable to predict the observed variation in barrier heights for a series of H atom transfer reactions.

In Figure 4, we compare observed barrier heights with reaction enthalpy. While there is a strong correlation within each homologous series involving a single radical, there is no correlation between reaction enthalpy and radical reactivity. For instance, barriers for X + ethane (connected with a dashed line in this and subsequent figures) go from nearly 5000 K for H to essentially 0 for Cl without any change in reaction enthalpy. They remain small (∼200 K) for Br (for the reverse reaction ethyl + HBr) in spite of a 10 kcal/mol change in reaction enthalpy, then rise slightly to ∼ 1000 K for OH, though the reaction is fully 20 kcal/mol exothermic. Reaction enthalpy, by itself, cannot explain radical reactivity for H atom transfer, and the failure is by no means unique to this system. For example, an examination of O atom transfer from ozone yields a similar result.

Covalent Curve Crossings. The singlet−triplet theory for barrier-height control in these reactions was treated by Pross et al.[35] As in the previous case, the authors compared a model with a computational result: in this case singlet−triplet splitting with electronic structure calculations (in most cases MP2/6--31G* //UHF/6--31G computations). The comparison between the singlet−triplet model and the ab initio calculations is satisfactory, but it does not stand up to the test of observations. The electronic structure calculations are neither accurate (barriers are up to a factor of 10 in error) nor precise (the fractional changes in barrier heights are much smaller than those observed, and reaction enthalpies are far off, by 16 kcal/mol in the case of methane + H → methyl + H_2). The authors conclude, however, that the singlet−triplet curve-crossing model explains the calculated variation in both symmetric RH + R reaction barriers and RH + H reaction barriers. To describe the calculated RH + Cl barriers, they include a significant perturbation from an ionic configuration.

Consider, however, a quantitative comparison with observations. In Figure 5 we compare observed barrier heights with the curve-crossing energy calculated using eq 9. Much as in the previous comparison, the calculation reasonably reproduces the observed trends for reactions involving a single radical, but fails to describe reactivity of a molecule with a series of radicals. In fact, the correlation is worse than before because eq 9 is relatively insensitive to the properties of the attacking radical. The radical enters into the theory only in the context of the bond being formed. If the properties of that forming bond do not change from one radical to the next, the predicted barrier height will not change. This is inconsistent with observations. A second problem can be seen by examining the changes of both barriers and crossing heights; both are of order 0.5 eV, so the slope of barrier height vs crossing height (to the extent that there is one) is of order 1:1, implying very weak coupling. Also, the entire range of barrier heights is compressed into a very small range of curve-crossing heights (0.5 eV in 3 eV).

Ionic Curve Crossings. Finally, we turn to the ionic curve-crossing theory. In Figure 6 we compare observed barrier

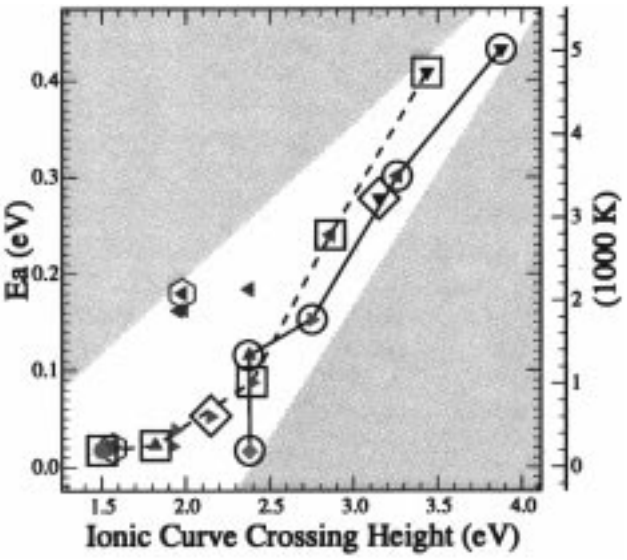

Figure 6. Observed barrier heights vs ionic curve-crossing energies. Symbols identify reactions as in Figure 3. Only with this theory do both molecular and radical reactivity progress along a common curve, with some tendency for larger alkanes to fall above the trend.

heights with the ionic curve-crossing energy calculated using eq 10. To produce this plot, we use a typical XH distance of 2.5 Å. This theory clearly captures the first-order behavior of the entire series of reactions. Not only is the general trend in both radical and molecule reactivity described, but the observed barriers all fall on a single, relatively tight line. The major deviation from this behavior is a tendency for barriers in larger alkanes to lie above the predicted trend. Furthermore, the slope of the correlation is much steeper than in the other cases, consistent with a strongly coupled avoided curve crossing.

The experimental evidence tests the zero-order involvement of the ionic surface. We conclude that ionic surfaces play the dominant role in governing barrier heights in these reactions. We turn now to the next level of detail to explore what happens at higher order.

Far Field Perturbations

The data strongly support our hypothesis that the ionic surface plays a controlling role in these reactions. However, we have relied on ad hoc assumptions about both the characteristic interaction distance and the evolution of both ground- and ionic-state energies. We shall combine low-level electronic structure calculations with an interaction analysis of the type described in Fukui[16] to constrain the interaction distance and to provide further insight into the evolution of both the ground- and ionic-state energies in the far field. We emphasize the far field, where the evolution of the ground and excited states proceeds with minimal overlap mixing between the reactants, because this locks in the curve-crossing boundary conditions. We emphasize both the ground and ionic states because the ground state, while the magnitude of its energy change is small, ultimately limits the interaction distance as it becomes repulsive.[25] For the ionic state we shall present a group of first-order perturbation terms depending on the charge distribution and polarizability of the vertically ionized reactants that cause the energy evolution to deviate from the simple Coulombic potential we have used so far.

Orbital Interactions. Though we shall focus on the far-field interactions, we shall begin by discussing a molecular-orbital picture of the atom-transfer problem itself. In Figure 7

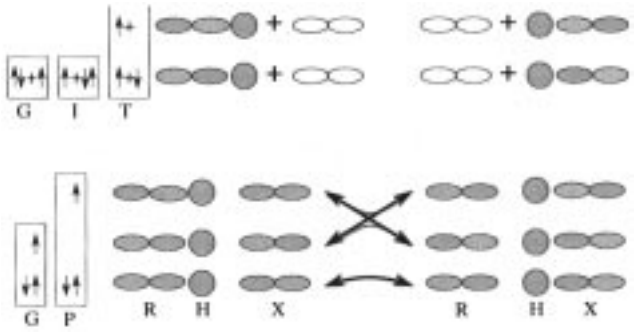

Figure 7. Hydrogen atom transfer orbitals and electronic configurations for three points during an abstraction reaction. Orbitals for separated reactants and products (Ψ_R and Ψ_P) are separate molecular orbitals, while orbitals near the transition state (Ψ_T) span the system. Orbital phase for the distant radicals is unimportant and thus not shown. Configurations for Ψ_R and Ψ_P are the ground state (**G**), with two electrons in the molecular HOMO and one electron in the radical SOMO, the ionic state (**I**), with one electron in the molecular HOMO and two electron in the radical SOMO, and the molecular triplet state (**T**), with one electron promoted to the molecular LUMO. **G** and **I** are the two lowest energy configurations when the reactants are proximate. The sketch for the transition-state wave function (Ψ_T) depicts the orbitals at two H atom positions, at the beginning and end of the atom transfer, and connecting arrows show the evolution of the orbital energies. Configurations for Ψ_T all have two electrons in the lowest energy MO. The third electron is forced into a higher energy orbital. Initially, the ground state (**G**) has a single electron in an orbital with positive overlap between R and H, and the promoted state (**P**) has a single electron in an orbital with positive overlap between H and X (this corresponds to the ionic configuration). As the hydrogen atom moves from R to X, these two configurations cross. The transition state is located at the crossing point.

we show molecular orbitals for the overall wave function at three points along the reaction coordinate, considering only orbitals generated from interactions of the singly occupied orbitals of the three radicals (R, H, and X). We assume that these SOMOs may be represented as a p, an s, and a p orbital, respectively. This choice is purely illustrative. Orbitals for separated reactants (Ψ_R) and separated products (Ψ_P) do not involve any interaction between the molecule and radical. For the separated species we show three configurations: the ground state, the ionic state, and the molecular triplet state. Near the transition state, however, the entire system constitutes a single macromolecule, and the wave function (Ψ_T) is more intricate.

The energies of the various molecular orbitals change rapidly as the H atom moves from one radical to the other. This is especially true for the orbitals into which the third of the three unpaired electrons is forced by the Pauli exclusion principle. The lowest lying molecular orbital has positive phase overlap near the H atom for all three atomic orbitals comprising it. It is highly delocalized and will be doubly occupied throughout the hydrogen transfer. The third electron is forced into a higher energy orbital. The second lowest lying orbital initially has positive overlap between R and H and negative overlap between H and X and corresponds to the ground state of RH + X. This orbital will be singly occupied during the beginning of the atom transfer. The third lowest lying orbital is the reverse of the second. As the atom exchange progresses, the second orbital energy rises while the third decreases; their crossing point approximately identifies the curve-crossing location. Therefore, the two key configurations for the atom exchange, labeled ground and promoted, differ only in which of the two partially bonding orbitals is occupied.

How do we correlate the configurations of the transition state with the configurations of the separated reactants? The

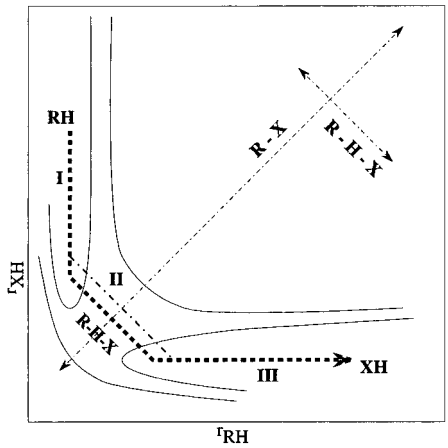

Figure 8. Approximate reaction coordinate for RH + X → R + XH, drawn on top of the ground-state surface for the R−H−X system. It develops in three stages: (I) approach of RH and X with no geometric distortion of either species, (II) transfer of H from R to X with R−X distance constant, (III) departure of XH from R, with no relaxation. The energy of the ground and ionic configurations along this coordinate develop as shown in Figure 2, with the boundary between the stages delineated by the dotted vertical lines.

promoted configuration does not obviously correspond to either the ionic or the triplet configuration of the separated reactants. In fact, it consists of a mixture of these two configurations. With extra electron density near the radical X, there is clearly charge separation associated with the ionic configuration; however, the antibonding nature of the R−H portion of the orbital wave function is associated with the triplet configuration. What enables us to identify this configuration is the asymptotic matching with the configurations of the separated species; in most cases the ionic configuration is lower in energy than the triplet configuration *once substantial overlap requires the macromolecular basis set.* Furthermore, the ionic configuration energy varies much more than the triplet configuration from reaction to reaction. Therefore, both the absolute magnitude and the change in the energy of the promoted configuration will be controlled by the ionic-state energy.

While one may perform a high-level configuration-interaction calculation on the transition-state macromolecule to find the transition-state geometry and energy, in practice this is impossible for all but the simplest systems. Furthermore, it obscures the essential simplicity of the problem. However, the physics of the configuration interaction itself is straightforward, provided one may constrain the boundary conditions. In this manner, the far-field evolution of the configurations appropriate to the separated reactants constrains and controls the overall problem.

This concept is directly related to the construction of a reaction coordinate. Figure 8 is a cartoon of the coordinate we apply, in which we break the reaction down into three stages corresponding to the approach of reactants, the transfer of the atom, and the separation of the products. Symmetry dictates that the first and third stages are similar. The coordinate is similar in concept to those presented earlier,[25,38] except that it is intentionally piecewise continuous. We confine all atomic rearrangement to the second stage, which allows us to use the approximate methods of Fukui with the greatest accuracy during the stages I and III. We use different physics to calculate the evolution of energies in stages I and III than we use in stage II, and we apply asymptotic matching to generate a smooth function.

Perturbation Treatment. To set up the initial-value problem for the curve crossing, we must model the evolution of the ground and electronic configurations while the reactants approach and the products separate. As long as the wave function resembles Ψ_R, the energies are easy to calculate. This holds true while the overlap between the reactant wave functions is small; the reactants remain essentially undistorted while long-range Coulombic and exchange forces (usually) increase the ground-state energy (E^G) and substantially decrease the ionic-state energy (E^I).

The ground-state energy evolves in the manner described by Fukui:[16]

$$E^G = E_K^G + E_Q^G \tag{11}$$

where E_K^G is the exchange energy and E_Q^G is the Coulombic energy. While the overlap between reactants is small, the coulombic term may be reasonably approximated by reducing electronic charges to the nuclei of each species.[16]

The ionic state initially lies at an energy (IP − EA) above the ground state but drops dramatically due to the strong ion−ion attraction:

$$E^I = (\mathrm{IP} - \mathrm{EA}) - E_i^I - E_{\rho,\alpha,\ldots}^I \tag{12}$$

where the ion−ion energy, E_i^I, is a simple charge−charge attractive potential $E_i^I = e^2/r$, and $E_{\rho,\alpha,\ldots}^I$ encompasses various near-field effects (ion charge distribution, anion polarizability, etc.).[39] The ionic-state energy drops until the overlap between reactant wave functions becomes large.

To cast the problem in a useful perturbative form, we make three zero-order assumptions: the ground-state Coulombic term is small ($E_Q^G \simeq 0$), all transition states for a given radical, *i*, form at roughly the same R−X distance, r_{T0i}, and the ions act as point charges. The first assumption is motivated by the consideration of atom−molecule reactions, while the second is based on extensive examination of radical−alkane reactions at the Hartree−Fock level of theory, where for example most OH transition states have $r_{T0} = 2.5$ Å, giving an ionic interaction energy of approximately 5.5 eV. Therefore, to zero order, we have

$$E_0^G = E_K^G(r_{T0}) \tag{13}$$

$$E_0^I = (\mathrm{IP} - \mathrm{EA}) - \frac{e^2}{r_{T0}} \tag{14}$$

These approximations, applied to both reactant and product ionic states, lead to the predicted crossing heights shown in Figure 6.

There are two aspects to consider at first order: so far we have neglected some contributions to both energies, and we have assumed a fixed interaction distance for each radical, r_{T0i}. As a first-order perturbation, we add the neglected terms and also consider the true transition-state interaction distance. The zero- and first-order terms are shown graphically in Figure 9. The interaction distance of the transition state on the ground state, r_T, differs from the nominal r_{T0}, and the appropriate interaction distance on the ionic state, r_{cc}, differs from r_T because the centers of charge of the virtual ionic state are not located on the R and X atoms. Given $\delta r_T = r_T - r_{T0}$ and $\delta r_{cc} = r_{cc} - r_{T0}$, the perturbation energy on the ground state is

$$E_1^G = \frac{\partial E_X^G}{\partial r}\delta r_T + E_Q^G(r_T) \tag{15}$$

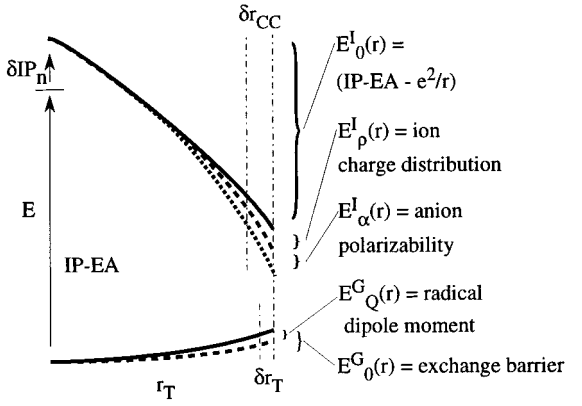

Figure 9. Perturbation terms to the ionic- and ground-state energies as the reactants approach. The ground-state energy (E_0^G) is influenced by Coulombic interactions ($E_Q^G(r_T)$). The ionic-state energy (E_0^I) is lowered by interactions with the charge distribution on each ion ($E_\rho^I(r_{cc})$) and by the polarizability of the radical anion ($E_\alpha^I(r_{cc})$). The initial ionic-state energy may be higher than the experimental IP − EA because the appropriate orbital to ionize may not be the HOMO (δIP_n).

where $E_Q^G(r_T) = E_Q^G(r_{T0}) + (\partial E_Q^G/\partial r)\,\delta r_T$, while the perturbation energy on the ionic state is

$$E_1^I = \delta IP + \frac{\partial E_i^I}{\partial r}\delta r_{cc} + E_\rho^I(r_{cc}) + E_\alpha^I(r_{cc}) \qquad (16)$$

where $E_\rho^I(r_{cc}) = E_\rho^I(r_{T0}) + (\partial E_\rho^I/\partial r)\,\delta r_{cc}$ and $E_\alpha^I(r_{cc}) = E_\alpha^I(r_{T0}) + (\partial E_\alpha^I/\partial r)\,\delta r_{cc}$. In eq 16, δIP is any difference between the ionic surface at infinite separation and IP − EA, including the role of ionic states other than the first ionic state, $E_\rho^I(r_{cc})$ is the energy due to the near-field charge distribution of the reactants (in the unoccupied, virtual, ionic states), and $E_\alpha^I(r_{cc})$ is the energy due to the polarizability of the reactants, again as virtual ions. The polarizability of the virtual anion is generally much greater than the polarizability of the virtual cation, so we consider only the former.

The terms in this treatment are all easily calculated. Specifically, the zero-order terms depend on easily measured properties of the separated reactants, while the first-order perturbation terms are either experimentally constrained or easily treated with low-level (UHF/6-31G**) ab initio calculations. The radical-specific interaction distances arising from this calculation are 2.3, 2.5, 2.5, 2.4, 2.8, and 3.0 Å for H, O, OH, F, Cl, and Br. One term in particular, δIP, deserves attention. In many cases the first ionization potential does not correspond to ionization out of a molecular orbital that develops overlap with the radical during the reaction. An example is ionization of the various radical−hydride product species, which serve as the electron donor in the reverse reaction. In all cases other than H_2, the HOMO is a lone pair that plays no role in the reaction. The appropriate IP correlates with an orbital containing significant electron density in the breaking bond. This correction also applies to the larger alkanes, where the HOMO electron density is largely along the carbon backbone.

Applying these first-order terms to the test set of reactions, we get the result displayed in Figure 10. The values are listed in the Appendix. The perturbation treatment has clearly improved the agreement between predicted curve-crossing energy and measured barrier heights. Now a single, nearly straight line describes the relationship for all reactions other than the H atom reactions, which lie slightly above the general trend. These include reactions spanning the entire space

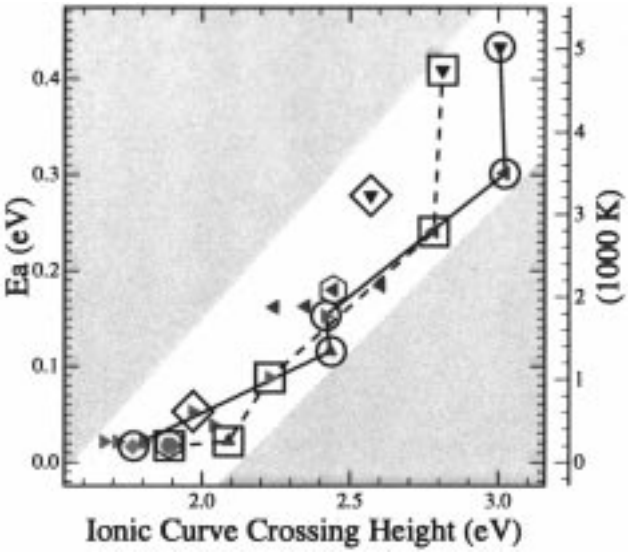

Figure 10. Observed barrier heights vs first-order ionic curve-crossing energies. Symbols identify reactions as in Figure 3. By accounting for specific Coulombic interactions of the reactants as well as the ionization potential of orbitals actually involved in the reaction, much of the deviation from a common trend seen in Figure 6 is removed.

described in Figure 3. The improvement with the higher order perturbation treatment is significant in itself, as it indicates that the data behave in a manner consistent with the theory. Finally, the slope (0.3) is consistent with strong coupling, though we expect the actual slope to change at higher order.

The two most significant terms are the charge distribution (dipole) term, which tends to steepen the curve by lowering the ionic-surface height for the smaller alkanes, and the IP term, which largely removes the curvature seen in Figure 6 for the larger alkanes. A more sophisticated treatment would include multiple ionic configurations in the larger alkanes, where degeneracy and a succession of closely spaced molecular orbitals complicate the problem.

One reaction in particular deserves attention. We have included the reaction ethyl + HBr → ethane + Br (a cyan circle in a square in the figures). There is currently some controversy about the experimental barrier for this reaction,[40,41] with some experiments showing a significantly negative activation energy and one a small positive activation energy. While we cannot resolve that discrepancy here, our theory does predict that the barrier should be quite low. In this case, the barrier is regulated by the ionic properties of the products and not the reactants. Specifically, the high electron affinity of Br makes the product ionic surface very low. This is an interesting class of reactions, with low crossings very late in the reaction coordinate, where the actual energy maximum may not be at the crossing point, or if the ionic-state energy is low enough, a stable intermediate could form.

Conclusions

We have shown that a configuration interaction between the ionic excited states and the ground state controls barrier heights in a large set of radical−molecule reactions. Other factors often cited as controlling influences, such as reaction enthalpy or the splitting between bonding and nonbonding configurations (the singlet−triplet gap), may play a role in determining the absolute barrier height, but the dominant property is the ionic-surface height (IP − EA).

In previous work,[23] we have discussed the interaction between the ionic and ground states as a stabilization of an intrinsic, or

TABLE 1: Modified Arrhenius Barrier Heights (in K)

alkane	OH	O	H
methane	1779 ± 10	3498 ± 10	5026 ± 12
ethane	1025 ± 10	2794 ± 7	4746 ± 5
propane	616 ± 5		3230 ± 9
n-butane	454 ± 6	2138 ± 9	
2-mepropane	257 ± 11		
n-pentane	414 ± 18	2002 ± 4	
n-hexane	284 ± 53		
cyclopentane	253 ±69	1889 ± 8	
cyclohexane	227 ± 43	2088 ± 7	
cycloheptane	256 ± 44	1880 ± 12	
cyclooctane	270 ± 62		

alkane	F	Cl	Br
methane	198 ±1	1340 ±1	
ethane		256 ±1	199 ±3

TABLE 2: Preexponentials (10^{-10} K^n cm^3 molecule^{-1} s^{-1})

alkane	OH[a]	O[b]	H[c]
methane	3.77 ± 0.14	0.26 ± 0.14	4.06 ± 2.09
ethane	11.63 ± 0.45	1.20 ± 0.49	33.17 ± 8.60
propane	13.18 ± 0.28		9.39 ± 4.32
n-butane	16.64 ± 0.37	3.57 ± 1.87	
2-mepropane	7.49 ± 0.29		
n-pentane	24.64 ± 1.51	5.55 ± 1.38	
n-hexane	21.01 ± 3.39		
cyclopentane	19.66 ± 4.13	7.40 ± 2.88	
cyclohexane	23.65 ± 3.11	15.21 ± 5.80	
cycloheptane	42.49 ± 5.86	15.84 ± 9.39	
cyclooctane	49.79 ± 10.02		

alkane	F	Cl	Br
methane	13.07 ± 1.47	1.15 ± 0.11	
ethane		19.84 ± 1.93	0.16 ± 0.03

[a] $\nu_1 = 280$ cm^{-1}, $\nu_2 = 500$ cm^{-1}. [b] $\nu_1 = 300$ cm^{-1}. [c] $\nu_1 = 600$ cm^{-1}. [d] $\nu_1 = 300$ cm^{-1}. [e] $\nu_1 = 400$ cm^{-1}. [f] $\nu_1 = 400$ cm^{-1}.

adiabatic, barrier by the overlying ionic state. This perspective is not far removed from that outlined by Shaik;[20] the intrinsic barrier can be viewed as a covalent barrier formed by the interaction of covalent electronic states (i.e., the singlet−triplet splitting), and the ionic surface can then be viewed as a perturbing agent responsible for supressing that adiabatic barrier. The strong correlation between observed barriers and the ionic properties of the reactants, operating as it does in many different radical−molecule systems, would then depend on a more or less constant adiabatic barrier for its coherence. Viewed in this context, there are two unifying questions to the overall problem: what controls the adiabatic barrier height, and what causes the large excursions of the observed barrier from the adiabatic barrier? The data shown in Figure 5 and Figure 6 suggest an answer to these questions. The adiabatic barrier for the reactions presented here is nearly constant, while the ionic states vary widely in energy, as do the observed barriers. While this formulation is consistent, it hides the essential controlling role of the ionic surface in these and many other reactions. The available excited states of like spin symmetry should be considered as a whole, once sufficient overlap forces a configuration interaction among them. We have shown that the ionic state is generally the lower energy state at this point, as well as being far more variable from system to system. The ionic curve-crossing model is therefore the appropriate zero-order model of barrier-height control for these systems.

Why do we care? Ultimately, a simple theory such as this should provide chemical insight. It is common, almost second nature, to assume that reaction enthalpy plays a dominant role in reactivity. Aside from the obvious constraint that the enthalpy provides a minimum barrier height, this assumption is not correct. More sophisticated curve-crossing models whose zero-order terms depend on the singlet−triplet gap can only describe radical reactivity by including a large perturbation from the ionic surface. This obscures the simplicity of what the data show us. The theory we present here shows clearly the observed progression of barriers and demonstrates the critical role of radical electron affinity in establishing radical reactivity. It is vital to have such conceptual theories. Agreement between experiments and high-level calculations is a triumph in the cases where it has been realized, but it is critical that a context be developed in which one can understand the simplicity of the physics governing the interactions, a context that stands up to the test of observations.

We wish to understand more complicated systems than the simple hydrogen transfer we have explored here. For instance, we need to understand why some reactions are direct and some are indirect. The covalent curve-crossing model and our ionic curve-crossing model may provide different insights into this issue; in all likelihood, there are domains in which one provides the correct first-order coupling scheme and other domains where the other theory applies. The two converge at higher order, where one considers the full configuration interaction. For the large class of radical−molecule reactions considered here, the most succinct first-order rule is that the lowest lying electronic excited state with the proper spin symmetry for either the reactants or products ultimately exerts the strongest control on the barrier height.

Acknowledgment. The work presented here is a continuation of a long chain of thought and research in our group over the past decade and more. It would have been impossible without the work, insight, and commentary of many past graduate students, including Lee Lowenstein, Randy Friedl, Darin Toohey, Phil Stevens, Fred Fenter, John Abbatt, Paul Wennberg, and Manvendra Dubey. We are in their debt. We also owe a great debt to the pioneering work of Kenichi Fukui. We thank two anonymous reviewers for insightful comments. This work was supported by NSF Grant 9414843 to Harvard University.

Appendix

Data. We have searched the literature extensively for temperature-dependent data on radical−alkane reactions with OH, O, H, and Cl. Data for OH reactions are taken from Atkinson[42] and references therein and more recent studies.[43,44] Our data-fitting procedure is discussed more completely in a companion paper.[44] Data for O atom reactions are from Herron[45] and references therein, data for H atom reactions are from NIST[46] and references therein, and data for Cl atom reactions are from JPL[47] and references therein. In addition, heats of formation and ionization energies are from NIST.[48]

To treat the curvature in Arrhenius plots caused by the transformation of rotations in the individual reactants into loose vibrations at the transition state, we use a modified Arrhenius form that explicitly incorporates the functional form of the rotational and vibrational modes, consistent with transition-state theory. We neglect tunneling effects. This is fully described in the companion paper.[44] For atom−molecule reactions we use the form

$$k(T) = \frac{B e^{-\mathrm{Ea}/T}}{(T^{1/2}(1 - e^{-1.44\nu_1/T})^2)} \qquad (17)$$

while for diatomic radical−molecule reactions we use the form

TABLE 3: First-Order Terms in the Ionic-State Energy Beyond the Zero-Order −5.5 eV Term

alkane	X	IP − EA	δ IP	$(\partial E/\partial r)\,\delta r$	E_ρ^I	E_α^I	E_1^I
methane	OH	10.78	0.00	−0.25	−0.33	−0.33	4.37
H_2O	methyl	12.54	1.78	−0.69	−0.99	−0.17	6.97
ethane	OH	9.73	0.00	0.33	−0.45	−0.22	3.89
H_2O	ethyl	12.88	1.78	−0.99	−0.65	−0.20	7.32
propane	OH	9.12	0.00	0.24	−0.41	−0.24	3.21
H_2O	isopropyl	12.94	1.78	−0.93	−0.47	−0.20	7.62
2-mepropane	OH	8.74	0.00	0.28	−0.71	−0.23	2.58
H_2O	tertbutyl	12.78	1.78	−0.20	−0.69	−0.12	8.05
n-butane	OH	8.70	0.47	0.29	−0.33	−0.22	3.41
H_2O	2butyl	12.74	1.78	−0.73	−0.54	−0.17	7.58
cyclopentane	OH	8.00	0.57	0.48	−0.35	−0.20	3.00
H_2O	cyclopentyl	12.62	1.78	−0.62	−0.66	−0.16	7.46
cyclohexane	OH	7.97	0.70	0.42	−0.26	−0.20	3.13
H_2O	cyclohexyl	12.62	1.78	−0.89	−0.19	−0.19	7.63
cycloheptane	OH	7.99	0.68	0.15	−0.26	−0.25	2.81
H_2O	cycloheptyl	12.62	1.78	−0.34	−0.77	−0.13	7.66
methane	O	11.15	0.00	−0.28	−0.34	−0.19	4.84
OH	methyl	12.94	3.18	−1.33	−1.28	−0.26	7.75
ethane	O	10.10	0.00	0.29	−0.47	−0.12	4.30
OH	ethyl	13.28	3.18	−1.70	−0.83	−0.32	8.11
n-butane	O	9.07	0.47	0.29	−0.33	−0.12	3.88
OH	2butyl	13.14	3.18	−1.39	−0.71	−0.27	8.45
cyclopentane	O	8.37	0.57	0.48	−0.35	−0.11	3.46
OH	cyclopentyl	13.02	3.18	−1.25	−0.82	−0.25	8.38
cyclohexane	O	8.34	0.70	0.42	−0.26	−0.11	3.59
OH	cyclohexyl	13.02	3.18	−1.58	−0.19	−0.33	8.60
cycloheptane	O	8.36	0.68	0.15	−0.26	−0.17	3.26
OH	cycloheptyl	13.02	3.18	−0.92	−0.98	−0.22	8.58
methane	H	11.86	0.00	−0.74	−0.43	0.00	5.19
H_2	methyl	15.34	0.00	−1.46	−1.14	−0.18	7.06
ethane	H	10.81	0.00	−0.06	−0.57	0.00	4.68
H_2	ethyl	15.68	0.00	−1.84	−0.68	−0.22	7.44
propane	H	10.20	0.00	−0.18	−0.52	0.00	4.00
H_2	isopropyl	15.74	0.00	−1.77	−0.45	−0.21	7.81
methane	F	9.21	0.00	−0.38	−0.36	−0.43	2.54
HF	methyl	15.95	2.97	−1.52	−1.29	−0.34	10.27
methane	Cl	9.00	0.00	0.47	−0.23	−0.40	3.34
HCl	methyl	12.67	4.05	−0.70	−1.32	−0.53	8.67
ethane	Cl	7.95	0.00	0.91	−0.32	−0.27	2.77
HCl	ethyl	13.01	4.05	−1.00	−0.96	−0.64	8.96
HBr	ethyl	11.94	3.82	−0.28	−0.83	−0.64	8.51
ethane	Br	8.20	0.00	1.16	−0.12	−0.58	3.16

$$k(T) = \frac{B e^{-Ea/T}}{(T(1 - e^{-1.44\nu_1/T})^2\,(1 - e^{-1.44\nu_2/T}))} \qquad (18)$$

In each case we assume that modes corresponding to bending vibrations of the heavy radical are degenerate. While this form is strictly appropriate only to single-channel reactions, we fit all of the available data with it, with excellent results. Both tunneling and multiple channels should be included in higher level treatments, such as the recent work on propane + OH branching.[49] However, the fitting procedure we use yields barriers unbiased by temperature (little change results by excluding high- or low-temperature data), so the effect of tunneling will be to generally raise the experimental barrier heights but not to alter the trends we analyze here.

While it is possible, in theory, to fit data for all of the free parameters in these functions, in practice this is imprudent. We constrain the frequencies in these functions with results from low-level ab initio calculations (UHF/6-31G**). Also, while we expect that the frequencies evolve along with the barrier heights in a given radical−alkane series, we do not wish to bias our data with any trends in the ab initio results. We therefore use a single set of frequencies for each radical. The resulting barrier heights (in K) are summarized in Table 1, while the preexponential (B) factors are summarized in Table 2. Note that we list the ethyl + HBr reaction as the reverse (Br + ethane) in the table to facilitate the presentation.

Perturbation Terms. The perturbation terms described by eq 16 are shown in Table 3 for the forward and reverse reactions treated in this paper. These terms are calculated by locating the transition state at a low level of ab initio theory (UHF/6-31G**) to find the interaction distance and then using charge distributions for the undistorted reactants computed at the same level of theory. The largest term (when it is nonzero) is the difference between the first ionization potential and the ionization potential appropriate to the reactive molecular orbital (δIP). Corrections for the difference between the true center of charge interaction distance and the zero-order 2.5 Å distance ($(\partial E/\partial r)\,\delta r$) as well as for the charge distribution of the reactants (E_ρ^I) are of similar magnitude. The effect of polarizability (E_α^I) is smaller but significant. The final ionic height (E_1^I) is shown in the last column. Note that most reactions are strongly asymmetric, with the reactant ionic surface much lower than the product surface. The exception is the HBr + ethyl reaction, where the product surface is much lower in energy.

References and Notes

(1) Christie, M. I.; Norrish, R. G. W.; Porter, G. *Proc. R. Soc. A* **1952**, *216*, 152.

(2) Morley, C.; Smith, I. W. M. *Trans. Faraday Soc.* **1972**, *68*, 1016.
(3) Wine, P. J.; Kreutter, K. D.; Ravishankara, A. R. *J. Phys. Chem.* **1979**, *83*, 3191.
(4) Herschbach, D. R. *Adv. Chem. Phys.* **1966**, *10*, 319.
(5) Lee, Y. T.; Gordon, R. J.; Herschbach, D. R. *J. Chem. Phys.* **1971**, *54*, 2410.
(6) Polanyi, J. C.; Woodall, K. B. *J. Chem. Phys.* **1972**, *57*, 1574.
(7) Kaufman, F. *Prog. React. Kinet.* **1961**, *I*, 1.
(8) Anderson, J. G.; Kaufman, F. *Chem. Phys. Lett.* **1972**, *16*, 375.
(9) Howard, C. J. *J. Phys. Chem.* **1979**, *83*, 3.
(10) Abbatt, J. P. D.; Demerjian, K. L.; Anderson, J. G. *J. Phys. Chem.* **1990**, *94*, 4566.
(11) Seeley, J. V.; Jayne, J. T.; Molina, M. J. *Int. J. Chem. Kinet.* **1993**, *25*, 571.
(12) Donahue, N. M.; Clarke, J. S.; Demerjian, K. L.; Anderson, J. G. *J. Phys. Chem.* **1996**, *100*, 5821.
(13) Porter, R. N.; Karplus, M. *J. Chem. Phys.* **1964**, *40*, 1105.
(14) Truhlar, D. G. Ed.. *Potential energy surfaces and dynamics calculations for chemical reactions and molecular energy transfer*; Plenum Press: New York, 1981.
(15) Allison, T. C.; Lynch, G. C.; Truhlar, D. G.; Gordon, M. S. *J. Phys. Chem.* **1996**, *100*, 13575.
(16) Fukui, K.; Fujimoto, H. *Bull. Chem. Soc. Jpn.* **1968**, *41*, 1989.
(17) Woodward, R. B.; Hoffman, R. *The Conservation of Orbital Symmetry*. Verlag Chemie: Weinheim, Germany, 1970.
(18) Gray, H. B. *Chemical Bonds: An Introduction to Atomic and Molecular Structure*; Benjamin Cummings: Menlo Park, 1973.
(19) Shaik, S. S.; Pross, A. *J. Am. Chem. Soc.* **1989**, *111*, 4306.
(20) Ṣhaik, S. S.; Hiberty, P. C. *Adv. Quantum Chem.* **1995**, *26*, 99.
(21) Ġusten, H.; Klasinc, L.; Marić, D. *J. Atmos. Chem.* **1984**, *2*, 83.
(22) Lowenstein, L. M.; Anderson, J. G. *J. Phys. Chem.* **1987**, *91*, 2993.
(23) Abbatt, J. P. D.; Toohey, D. W.; Fenter, F. F.; Stevens, P. S.; Brune, W. H.; Anderson, J. G. *J. Phys. Chem.* **1989**, *93*, 1022.
(24) London, F. *Z. Phys.* **1928**, *46*, 455.
(25) Evans, M. G.; Polanyi, M. *Trans. Faraday Soc.* **1938**, *34*, 11.
(26) Sato, S. *J. Chem. Phys.* **1955**, *23*, 592.
(27) Marcus, R. A. *J. Chem. Phys.* **1956**, *24*, 966.
(28) Marcus, R. A. *J. Phys. Chem.* **1968**, *72*, 891.
(29) Pross, A. *Adv. Phys. Org. Chem.* **1985**, *21*, 99.
(30) Yasumori, I. *Bull. Chem. Soc. Jpn.* **1959**, *32*, 1103.
(31) Silver, D. M. *J. Am. Chem. Soc.* **1974**, *96*, 5959.
(32) Pross, A. *Theoretical and Physical Principles of Organic Reactivity*; John Wiley and Sons: New York, 1995.
(33) Garrett, B. C.; Truhlar, D. G. *J. Chem. Phys.* **1985**, *82*, 4543.
(34) Shaik, S. S.; Hiberty, P. C.; Lefour, J.-M.; Ohanessian, G. *J. Am. Chem. Soc.* **1987**, *109*, 363.
(35) Pross, A.; Yamataka, H.; Shigeru Nagase. *J. Phys. Org. Chem.* **1991**, *4*, 135.
(36) Kreevoy, M. M.; Truhlar, D. G. In *Investigation of Rates and Mechanisms of Reactions*; Bernasconi, C. F., ed.; John Wiley and Sons: New York, 1986; Vol. VI, p 13.
(37) Dubey, M. K.; Mohrschladt, R.; Donahue, N. M.; Anderson, J. G. *J. Phys. Chem.* **1997**, *101*, 1494.
(38) Marcus, R. A. *Discuss. Faraday Soc.* **1967**, *44*, 7.
(39) Rittner, E. S. *J. Chem. Phys.* **1951**, *19*, 1030.
(40) Nicovich, J. M.; van Dijk, C. A.; Kreutter, K. D.; Wine, P. J. *J. Phys. Chem.* **1991**, *95*, 9890.
(41) Dobis, O.; Benson, S. W. *J. Phys. Chem.* **1997**, *101*, 6030.
(42) Atkinson, R. *J. Phys. Chem. Ref. Data* **1994**, Monograph 2.
(43) Talukdar, R. K.; Mellouki, A.; Gierczak, T.; Barone, S.; Chiang, S-Y; Ravishankara, A. R. *Int. J. Chem. Kin.* **1994**, *26*, 973.
(44) Donahue, N. M.; Anderson, J. G.; Demerjian, K. L. *J. Phys. Chem. A* **1998**, *102*, 3121.
(45) Herron, J. T. *J. Phys. Chem. Ref. Data* **1988**, *17*, 967.
(46) Mallard, W. G. NIST chemical kinetics database. Technical Report 17, NIST, **1994**.
(47) DeMore, W. B.; Sander, S. P.; Golden, D. M.; Hampson, R. F.; Kurylo, M. J.; Howard, C. J.; Ravishankara, A. R.; Kolb, C. E.; Molina, M. J. Chemical kinetics and photochemical data for use in stratopsheric modeling. Technical Report 97-4, Jet Propulsion Laboratory, **1997**.
(48) Mallard, W. G. NIST chemistry webbook. Technical Report 69, NIST, **1997**. http://webbook.nist.gov/.
(49) Hu, W. P.; Rossi, I.; Corchado, J. C.; Truhlar, D. G. *J. Phys. Chem.* **1997**, *101*, 6911.